Preparation of Nano Poly(phenylsilsesquioxane) Spheres(nano-PPSQ) and Study of the Thermal Stability and Crystallization Behavior of PP/Nano-PPSQ Composites

Xinlong Wang, Jin Li, Lianghu Wu

Department of Polymer, School of Chemical Engineering, Nanjing University of Science and Technology, Nanjing 210094, China

Received 21 July 2010; accepted 3 November 2010
DOI 10.1002/app.33691
Published online 25 February 2011 in Wiley Online Library (wileyonlinelibrary.com).

ABSTRACT: The preparation of nano poly(phenylsilsesquioxane) particles (nano-PPSQ) and the influence of nano-PPSQ on the thermal stability and crystallization of polypropylene (PP) were studied. The morphology and thermal stability of PP/nano-PPSQ composites were characterized by scanning electron microscopy (SEM) and the thermogravimetric analysis (TGA). The SEM result showed that the particles were well dispersed in the PP matrix. The TGA results of the PP/nano-PPSQ composites indicated that the incorporation of nano-PPSQ can improve the thermal stability of PP. The crystallization behavior and kinetics of PP/nano-PPSQ composite were studied by X-ray diffraction (XRD) and differential scanning calorimetry (DSC). The XRD revealed that the addition of nano-PPSQ influences the crystallinity and crystal size of PP. The Avrami, Ozawa, and combined Avrami/Ozawa (Mo method) equations were applied to describe the crystallization kinetics and estimate the kinetic parameters of mathematical models under the nonisothermal crystallization of PP and PP/nano-PPSQ composites. The results show that nano-PPSQ influences the crystallization temperature and rate. © 2011 Wiley Periodicals, Inc. J Appl Polym Sci 121: 995–1003, 2011

Key words: poly(phenylsilsesquioxane); nano particles; PP; thermal stability; nonisothermal crystallization

INTRODUCTION

Recently, there has been considerable interest in the development of organic–inorganic hybrid materials because of their broad potential applications including battery electrolytes, food packaging, dental and bone implants, and materials used for controlled chemical release.[1,2] Organic–inorganic hybrid material in which the organic components are bonded to a siloxane or silica backbone, are variously referred to as organically modified silicas, ormosils, or silsesquioxanes. Considerable attention has focused on the synthesis of this class of hybrids owing to the unique possibilities to combine the properties of the organic moieties with those of the siloxane or silica matrix.[3–5] The presence of organic groups also renders the surface of the particles more hydrophobic than that of inorganic particles, thus offering the potential to improve compatibility between the filler and the host polymer. Poly(phenylsilsesquioxane) (PPSQ) is the most investigated polymer of the silsesquioxane class because of its good thermal stability. Potential applications of this polymer include lithographic materials, gas-separation membranes, coatings for electronic and optical devices, especially where high temperatures are required.[6] Over the past decade, polymer nanocomposites have received considerable attention as an effective way to develop new composite materials. Nanocomposites are a new class of composites that are particle-filled polymers for which at least one dimension of the dispersed particles is in the nanometer range. At this scale, the inorganic fillers improve sharply the properties of polymer due to the nanoscale structure of the hybrids.[7] As it is the case for semicrystalline polymers, thermal and mechanical properties of PP composites depend on the crystallinity degree. Such information leads to the understanding of crystallization kinetics in semicrystalline polymer systems which in turn control their mechanical and other engineering properties.[8] In this article, the nano poly (phenylsilsesquioxane) particles (nano-PPSQ) having uniform size distribution were prepared and the thermal stability and crystallization of PP/nano-PPSQ composites were investigated to study the influence of nano-PPSQ on them.

Correspondence to: X. Wang (wxinlong@sohu.com).
Contract grant sponsor: National Natural Science Foundation of China; contract grant number: 20473038.
Contract grant sponsor: Natural Science Foundation of the Education Committee of Jiangsu province; contract grant number: 04KJB150066.

EXPERIMENTAL

Materials

Phenyltrimethoxysilane (PTMS, Aldrich) was used as received. Emulsifier TX-10 (alkylphenol polyoxyethylene(10) ether, $M_W = 646$, chemical purity), acetic acid and methanol of analytical reagent quality were purchased from Chemical Reagent Limited Corp. of National Medicine Group, China. Polypropylene (Type 1400, The $\overline{M}_w$ is about 60,000 g/mol, MFI is 3.4 g/10 min, density is 0.910 g/cm^3, tacticity is 96.0%, degree of crystallinity is about 60% by DSC) was supplied by Nanjing Yangzi Plastic Corp., China.

Preparation of nano poly(phenylsilsesquioxane) particles

In a 250-mL round bottom flask fitted with a stirrer, 100 g aqueous solution of NaOH (pH = 12.5) and 1 g TX-10 were added. The mixture was heated to 50°C and 5 g of PTMS were carefully added dropwise with a stirring speed of 300 rpm for 30 min to ensure uniformity of the mixture. After stirring continuously for another 2.5 h at 50°C, the mixture was cooled to room temperature and 3 g aqueous solution of acetic acid (wt 10%) were added. The product was collected by filtration and washed three times with 100 mL deionized water and one time with 50 mL methanol. The resulting product was dried in a vacuum oven for 4 h at 60°C.

Preparation of PP/nano-Ppsq composite samples

The nano poly(phenylsilsesquioxane) particles was blended with powdered PP by melt mixing in an internal mixer (60 cc, Haake Polydrive 600) at 180°C and 50 rpm for 10 min. The mixture was into pellets, dried and injection molded into various specimens at 200°C for testing.

Analysis procedure

The morphology of nano poly(phenylsilsesquioxane) particles was characterized by a JEOL-2100 transmission electron microscope (TEM) apparatus (Electronic Corp., Japan). IR spectra were recorded on an FTIR-8400S (Shimadzu Corp., Japan) using KBr discs. The X-ray diffraction analysis was recorded on a D8 ADVANCE Apparatus (Bruker) using Cu (Ka) radiation. The morphologies of PP and PP/nano-PPSQ composites were observed by a Philips XL-305 FEG-SEM instrument. The thermal stability of PP and PP/nano-PPSQ composites was measured by nonisothermal thermogravimetry method using a DTG-60/60H Simultaneous DTA-TG Apparatus (Shimadzu Corp., Japan) from room temperature to 600°C at a heating rate 20°C/min in nitrogen atmosphere or air in a flow rate of 20 mL/min. Differential scanning calorimetry (DSC) measurement was investigated in a nitrogen atmosphere using a Q80 DSC Apparatus (TA Corp., America). The samples were heated from 50 to 210°C at a heating rate of 20°C/min and then kept at 200°C for 5 min to eliminate previous thermal history. Then, the samples were cooled at cooling rates of 5, 10, 20, and 40°C/min, respectively.

RESULTS AND DISCUSSION

Preparation and characterization of nano poly(phenylsilsesquioxane) particles

The preparation of silica spheres has received considerable attention because of the development of the Stöber method, which gives rise to submicron monodisperse spherical silica particles.[9,10] The key reaction parameters responsible for the control of size and morphology of the particles can be effectively controlled by changing the reaction conditions such as the organoalkoxysilanes ratio and agitation. The morphology of the prepared particles was characterized by transmission electron microscopy (see Fig. 1). The spheres with a diameter of about 100 nm were prepared by the 5 : 100 weight ratio of PTMS and water with a yield of about 90%.

Figure 2 shows FT-IR spectrum of the nano-PPSQ particles. The OH functionality existing is visible as the broad absorption from 3144.0 cm^{-1} to 3746.0 cm^{-1}. Peaks at 3073.0 cm^{-1} and 3048.0 cm^{-1} are due to the C—H stretching vibration in

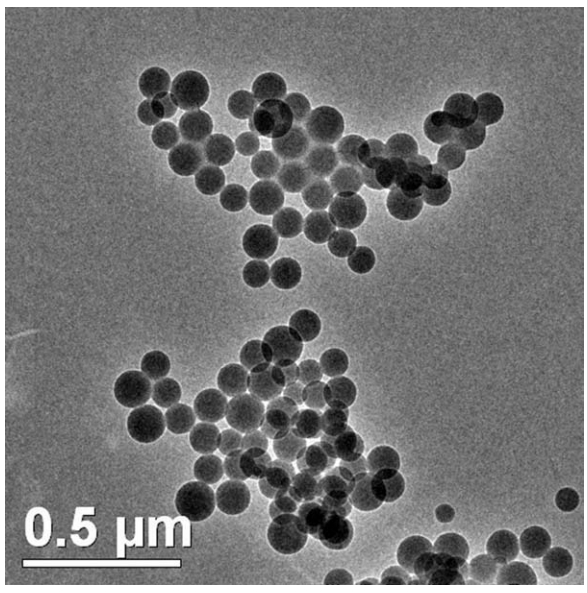

Figure 1 TEM micrograph showing the morphology of the prepared nano-PPSQ particles (5% of PTMS in 100% of water).

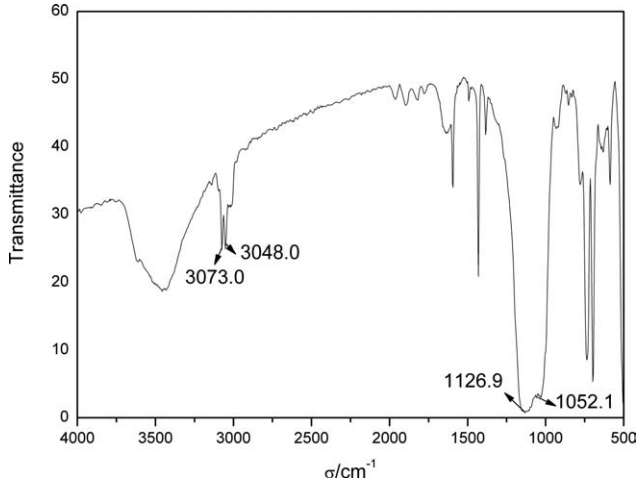

Figure 2 FTIR spectrum of the nano-PPSQ particles.

the phenyl group on the particles. A strong broad band at 1126.9 cm^{-1} and 1052.1 cm^{-1} resulting from Si—O—Si stretching is observed clearly in the prepared particles. It was reported that the characteristic vibrations, Si—O—Si asymmetric stretching was present at 1100–1140 cm^{-1} or 1057–1085 cm^{-1} in the cases of strained geometry. For example, the band for a T8 was reported at 1121 cm^{-1}, and it was slightly shifted to 1128 cm^{-1} for a T10. Strained cycles as those present in a T6 showed the band at 1051–1057 cm^{-1}. Therefore, it is reasonable to consider that the nano-PPSQ particles obtained are a mixture of these species.[11]

Figure 3(a) shows the XRD spectra of the nano-PPSQ particles. The relatively sharp peak at around 7.6° and the broad peak at around 19.4° can be ascribed to the chain-to-chain distance and the intrachain distances for a stereoregular double-chain structure respectively. The peak in the small-angle region is sharp and intense, indicating that the particles possessed high regularity structure, it was estimated that the chain-to-chain distance and intrachain distances in the prepared particles were 1.2 nm and 0.6 nm, respectively.[6]

SEM analysis of nanocomposites

The formulations of the nanocomposite are listed in Table I. The dispersion of the particles is very important for the nanocomposite properties. SEM micrographs showing morphology of PP and nanocomposites are given in Figure 4(a,b) respectively. No large aggregates are present and this shows the good dispersion of particles in the PP matrix. It can be explained that phenyl groups render the surface of the particles more hydrophobic and thus improve compatibility between the filler and PP.

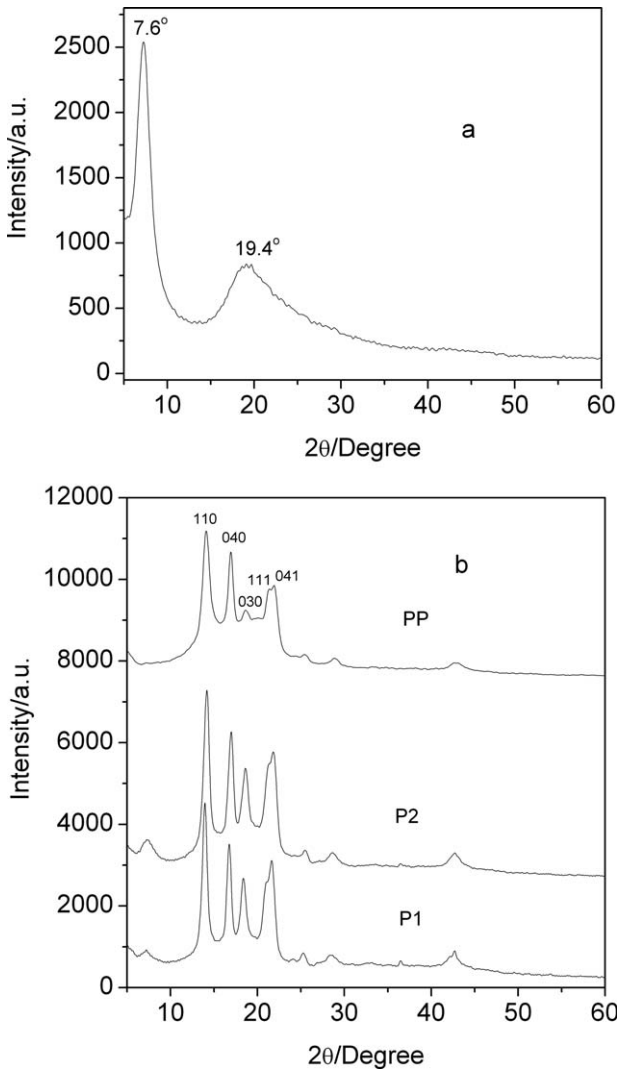

Figure 3 XRD patterns: (a) the nano-PPSQ particles, (b) pure PP and nanocomposites.

Thermal stability of nanocomposites

Figure 5(a,b) shows the TGA curves of nanocomposites in nitrogen and air flow. The curves of all samples show one step of weight loss. The data including the temperature at which 10% weight loss occurs (T_{10}, a measure of onset temperature of degradation) and the temperature for 50% degradation

TABLE I
The Formulations and TGA Data for PP and PP/Nano-PPSQ Composites (P1 and P2) Under Nitrogen and Air Atmosphere

			Nitrogen		Air	
Samples	PP (wt%)	Nano-PPSQ (wt%)	T_{10} (°C)	T_{50} (°C)	T_{10} (°C)	T_{50} (°C)
PP	100	0	341.9	423.3	315.2	397.0
P1	95	5	401.5	452.5	337.4	423.4
P2	90	10	405.5	454.3	338.1	419.0

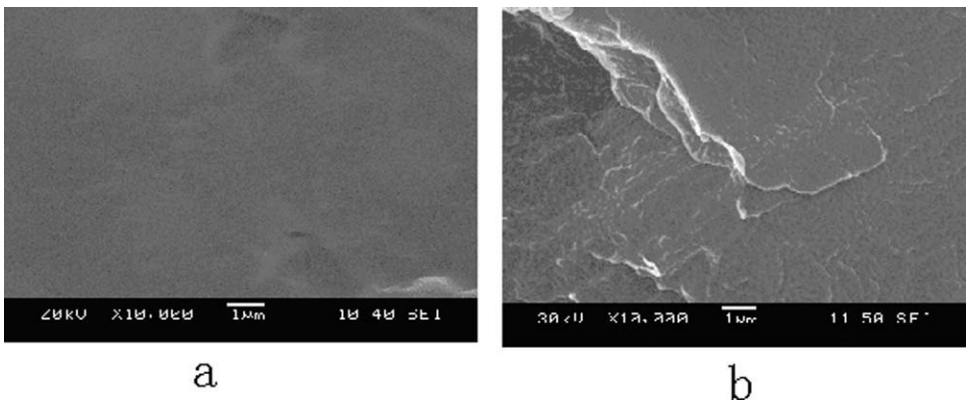

Figure 4 SEM micrographs: (a) pure PP and (b) nanocomposite P2.

(T_{50}) as the mid-point of degradation are used to evaluate the thermal stability and are listed in Table I. Tests made in the nitrogen showed that T_{10} and T_{50} of the PP started at 341.9°C and 423.3°C, while the T_{10} and T_{50} of the composites with wt 5% nano-PPSQ started at 401.5°C and 452.5°C, respectively. A significant difference in these degradation temperatures, initiated under nitrogen, 59.6°C and 29.2°C, respectively, indicates a thermal stability improvement probably due to hindered out-diffusion of the volatile products in the presence of the nano-PPSQ particles. Similar to the results in nitrogen, the composites containing nano-PPSQ have a higher decomposition temperature in contrast to the pure PP under air atmosphere indicating that oxygen diffusion in the composite is impeded.[12]

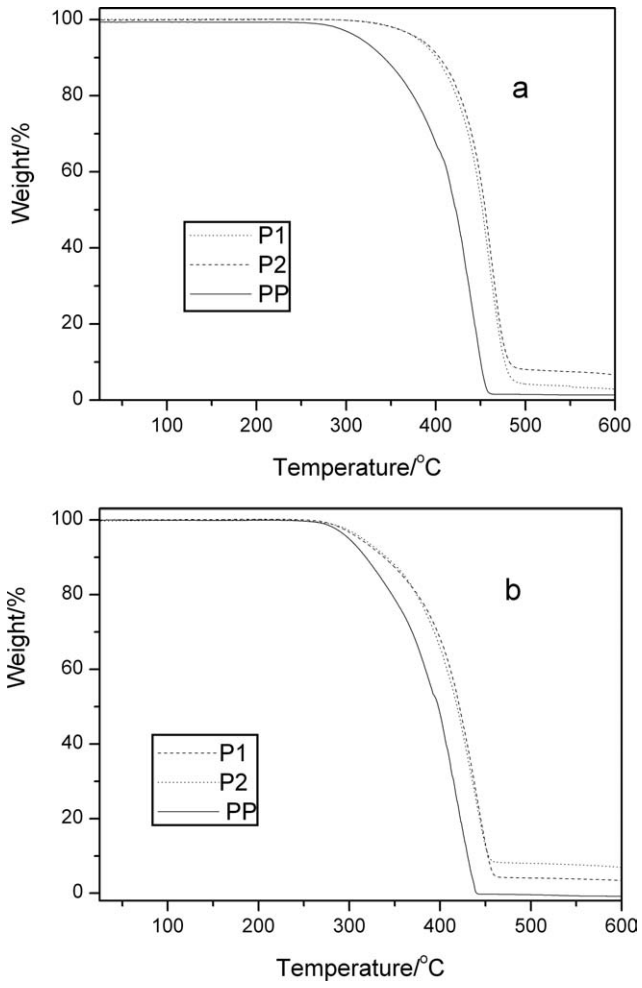

Figure 5 TGA curves of PP, P1, and P2 samples in nitrogen (a) and air (b).

Crystallization behavior of nanocomposites

PP is capable of crystallizing in three polymorphic forms, α (monoclinic), β (pseudohexagonal), and γ (triclinic), depending on the composition of PP and the crystallization conditions. The diffraction peaks at 14.0, 16.8, 18.5, 21.0, and 21.8° corresponded to α (110) α (040) α (130) and overlapping α (111) and α (131) reflections, respectively, whereas the diffraction peaks located at 16.1 and 20.1° belonged to the β (300) and γ (117) planes in XRD patterns.[13] The XRD patterns of pure PP and the nanocomposites are shown in Figure 3(b). Characteristic peaks of the PP a-phase are observed in composites. The PP and the composites show the same reflections and this indicates that presence of the nano-PPSQ particles does not affect the crystallographic nature of PP. Another feature that can be observed in Figure 3(b) is the relative intensity and the width of peaks. The change in intensity and breadth of reflections is an indication of crystal orientation.[14] From the results shown for α_1(110) α_2(040) α_3(130), and α_4(111) it is clear that all the peaks in the composite with the nano-PPSQ particles are more intense and wider than those of pure PP. This means that the addition of nano-PPSQ particles influences the crystallinity and crystal orientation of PP.

On the basis of the Scherrer equation,

$$D_{hkl} = k\lambda/(\beta \cos \theta)$$

TABLE II
Crystallite Size D_{hkl} of PP and PP/Nano-PPSQ Composites

Sample	Crystallite size(nm)				
	L_{110}	L_{040}	L_{130}	L_{111}	L_{041}
PP	20.09	34.10	18.59	15.46	30.93
P1	23.77	25.10	16.74	13.26	22.09
P2	21.04	20.46	18.12	8.64	15.55

where D_{hkl} is the crystallite size perpendicular to reflection plane (hkl) (nm), k is a shape factor of crystallite size (0.89), λ is the wavelength of X-ray used(nm), β is the width of diffraction beam used (rad), and θ is the Bragg angle. Crystallite size D_{hkl} of PP and nanocomposites are summarized in Table II. As it can be seen in Table II, crystallite size perpendicular to the crystal plane like (0 4 0), (1 1 1), (0 4 1) in nanocomposites was smaller than that of PP. This clearly indicated that crystallite size of nanocomposites decreased by introducing nano-PPSQ particles. During crystallization of PP from melt, nano-PPSQ particles act as heterogeneous nucleating agent and are inclined to absorb macromolecule segments. Therefore, the movement of the macromolecule segments is constrained and crystallization is initiated. Because of the existence of nuclei, the spherulite cannot grow large enough to overlap due to the very fast nucleation rate. Accordingly, the size of spherulites in nanocomposites would be smaller than those in pure PP.

Nonisothermal crystallization kinetics of nanocomposites

Nonisothermal crystallization, the common industrial route, is much more complicated than isothermal situation due to alteration of thermal environment with time. The crystallization exotherms of PP and nanocomposites at different cooling rates are presented in Figure 6(a–c). From these curves, the peak temperature (T_p) can be obtained for describing the nonisothermal crystallization and are listed in Table III(Φ is the cooling rate). T_p shifts to lower temperature with increasing cooling rate. This can be explained by the fact that lower time scale will affect the polymer to crystallize and the polymer requires a higher undercooling to initiate crystallization. Besides, the motion of PP molecules cannot follow the cooling temperature when the specimens are cooled fast. For a given cooling rate, T_p of the nanocomposites are higher than that of pure PP, and this can be attributed to the fact that the nanocomposites have heterogeneous nucleation effects on PP macromolecule segments.[15] This accords well with XRD results.

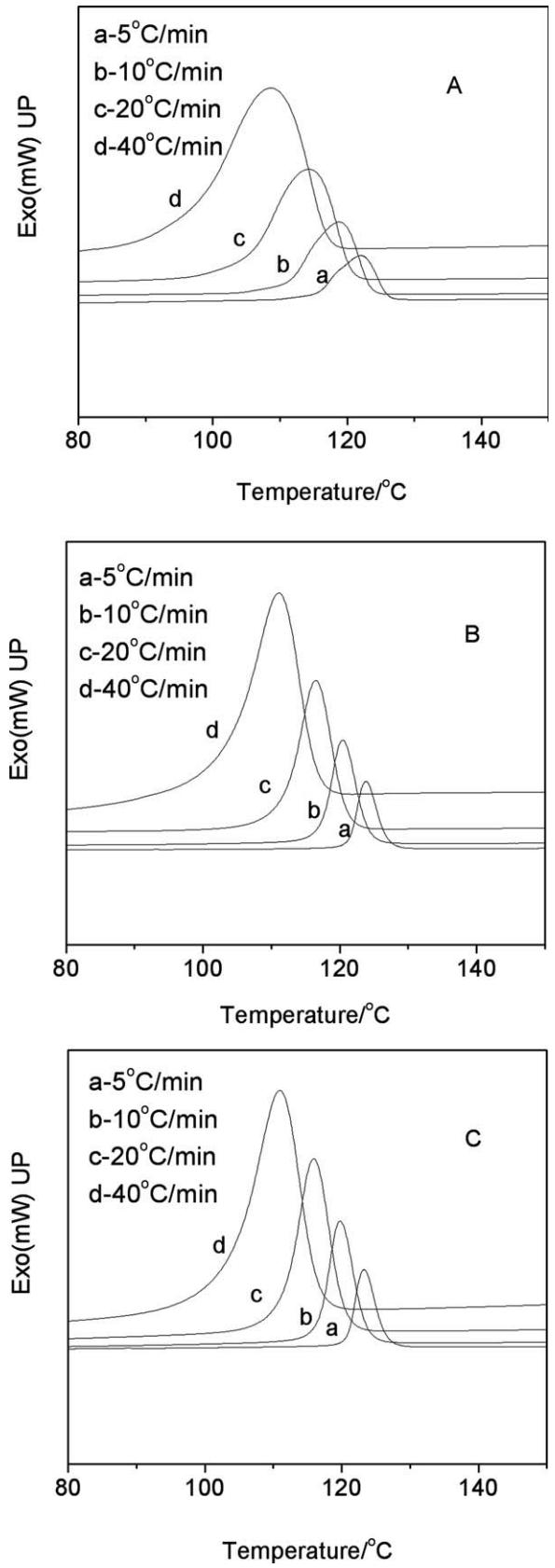

Figure 6 DSC curves in nitrogen for different cooling rates: (a) PP, (b) P1, and (c) P2.

TABLE III
Kinetic Parameters of Nonisothermal Crystallization for PP and PP/Nano-PPSQ Composites

Samples	Φ (°C/min)	T_p (°C)	$t_{1/2}$ (min)	Z_c	n	R
PP	5	122.0	1.40	0.73	2.80	0.99721
	10	118.8	0.79	0.71	2.69	0.98787
	20	114.3	0.50	0.77	2.729	0.98889
	40	108.6	0.33	0.66	2.81	0.99178
P1	5	123.3	1.33	0.99	3.34	0.98811
	10	119.8	0.76	1.02	3.24	0.99016
	20	115.9	0.44	1.03	3.36	0.99604
	40	110.9	0.28	1.01	3.18	0.99001
P2	5	123.8	1.28	1.06	3.38	0.98783
	10	120.4	0.75	1.11	3.39	0.98975
	20	116.4	0.44	1.11	3.39	0.99372
	40	111.0	0.28	1.08	3.18	0.98868

The relative degree of crystallinity, X_t, as a function of crystallization temperature T is defined as:

$$X_t = \int_{T_0}^{T} (dH/dT)dT / \int_{T_0}^{T_\infty} (dH/dT)dT \quad (1)$$

where T_0 and T_∞ represent the onset and end of crystallization temperatures respectively. The crystallization temperatures during cooling can be converted to crystallization time using eq. (2),

$$t = (T_0 - T)/\Phi \quad (2)$$

where t is crystallization time, T_0 the onset crystallization temperature, T the temperature at crystallization time at t, and Φ the cooling rate from melt state. The relative crystallinity of pure PP and nanocomposites can be expressed as a function of crystallization time, as shown in Figure 7(a–c). It can be seen that all these curves have the same sigmoidal shape, which means that only the lag effect of cooling rate on crystallization is observed. Figure 7(a–c) also shows that the higher the cooling rate is, the shorter the time for completing crystallization is. The half-time of nonisothermal crystallization $t_{1/2}$ could be obtained from Figure 7(a–c) and the results are listed in Table III. The values of $t_{1/2}$ decrease with increasing cooling rates and at a given cooling rate, the values of $t_{1/2}$ for the nanocomposites are smaller than that of PP. This indicates that that the addition of nano-PPSQ can accelerate the overall crystallization process.

Avrami equation

The Avrami equation can be applied to describe the initial stage of crystallization under nonisothermal crystallization as follows[16]:

$$1 - X_t = \exp(-Z_t t^n) \quad (3)$$

where X_t is the relative degree of crystallinity at time t. Both the parameter Z_t and the Avrami exponent n are diagnostic of the crystallization mechanism. The Avrami exponent n describes the growing mechanism and geometry of crystallization, and the parameter Z_t describes the growth rate in the nonisothermal crystallization process. The double-logarithmic form of the above Avrami equation yields:

$$\ln[-\ln(1 - X_t)] = \ln Z_t + n \ln t \quad (4)$$

According to Jeziorny model, the constant $ln\ Z_t$ can be expressed as:

$$\ln Z_c = \ln Z_t/\varphi \quad (5)$$

where Z_c is the corrected Jeziorny crystallization constant.[17] According to eqs. (3) and (4), the plot of ln[−ln(1−X_t)] versus lnt will give the slope n, the Avrami exponent, and the intercept lnZ_c, as shown in Figure 8(a–c) and Table III. As listed in Table III, the n values of nanocomposites and pure PP are about 3.00 ± 0.40. Normally, n values close to 3 indicate an athermal and sporadic nucleation process followed by three-dimensional crystal growth. The parameter Z_c describes the crystallization rate of the polymer molecules and the value of Z_c increases with increasing cooling rates. The values of Z_c for nanocomposites are larger than that for PP at a given cooling rate, implying that nanocomposites finished crystallization process at a quicker speed than PP.[18]

The Ozawa method

Ozawa developed a new extended form of Avrami equation to determine the crystallization parameters and dimensional growth. eq. (6) was proposed for the investigation of nonisothermal crystallization kinetics by integration of infinitesimally small isothermal crystallization steps:

$$\ln[-\ln(1 - X_t)] = \ln K(\mathrm{T}) - m \ln \Phi \quad (6)$$

where $K(T)$ is a crystallization constant, and m is Ozawa parameter related to the crystal dimensional growth. Figure 9(a–c) shows the nonisothermal crystallization

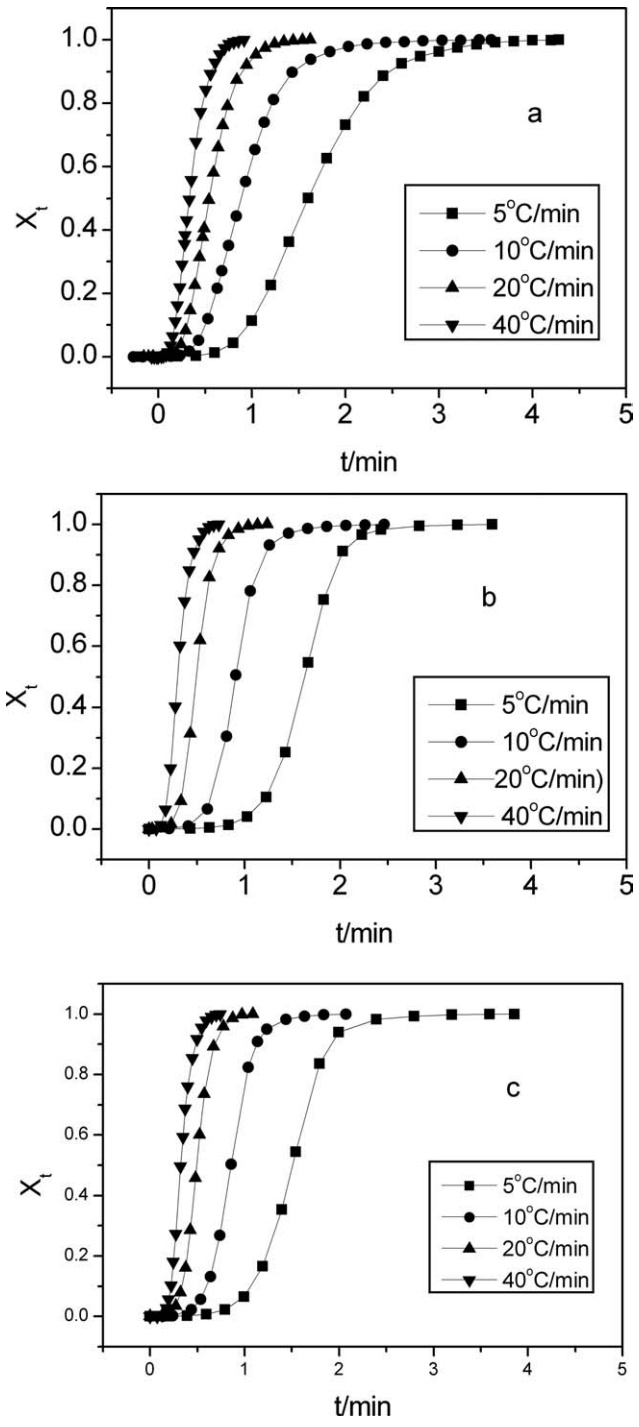

Figure 7 Plots of X_t at different cooling rates: (a) PP, (b), P1 and (c) P2.

results of samples according to Ozawa's method at 108, 110, 112, 114, 116, and 118°C. The curvature in Figure 9 prevents an accurate analysis of nonisothermal crystallization data. The Ozawa method does not take into account the difference caused by the time and the cooling rate. Some studies have predicted other disregarded factors such as the folded chain length of the polymer chain and the secondary crystallization in the Ozawa method.[19]

The Mo method

Mo combined the Avrami n and Ozawa m exponents and derived another form of kinetic equation as given below[20]:

$$\ln \Phi = \ln F(T) - \alpha \ln t \tag{7}$$

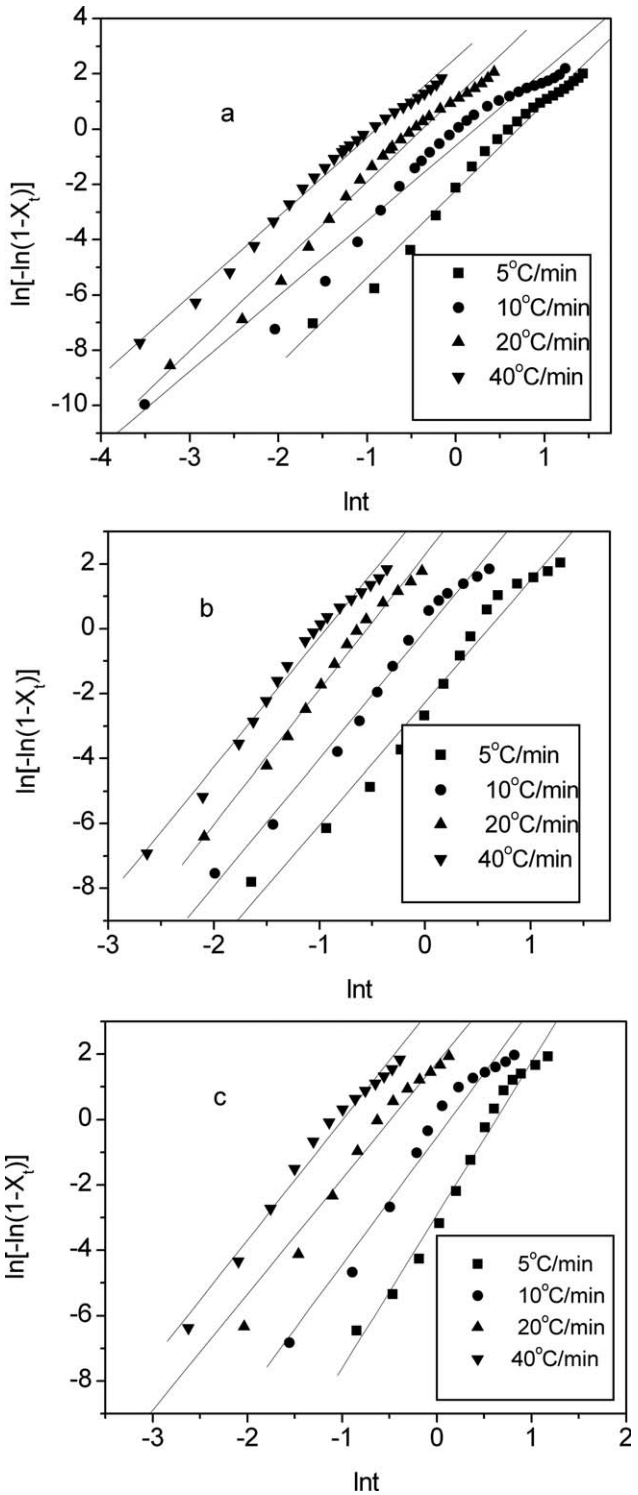

Figure 8 Plots of $\ln[-\ln(1-X_t)]$ versus lnt at different cooling rates: (a) PP, (b) P1, and (c) P2.

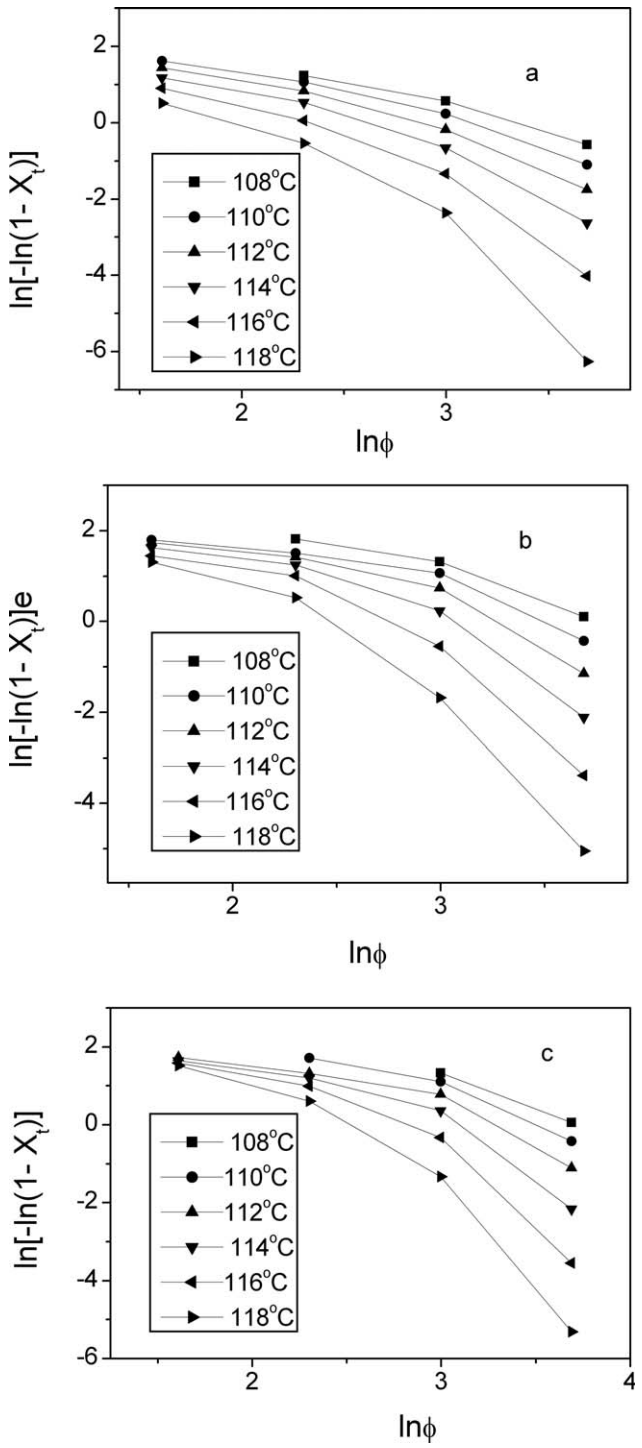

Figure 9 Plots of $\ln[-\ln(1-X_t)]$ versus $\ln\Phi$ (according to Ozama's method) : (a) PP, (b) P1, and (c) P2.

where $F(T)$ is the crystallization constant, a is the ratio of n and m exponents related to the crystallization dimension. The plots of $\ln\Phi$ versus lnt using eq. (7) at a given degree of theoretical crystallinity are shown in Figure 10(a–c), and straight lines are obtained for the three cases. Values of α from the slopes and of $F(T)$ from the intercepts are given in Table IV. The $F(T)$ increases with the degree in crystallinity for PP as well as for the nanocomposites. When the values of crystallinity are above 20%, the $F(T)$ values of nanocomposites are smaller than that of neat PP, indicating that the crystallization rates are faster in the presence of nano particles.

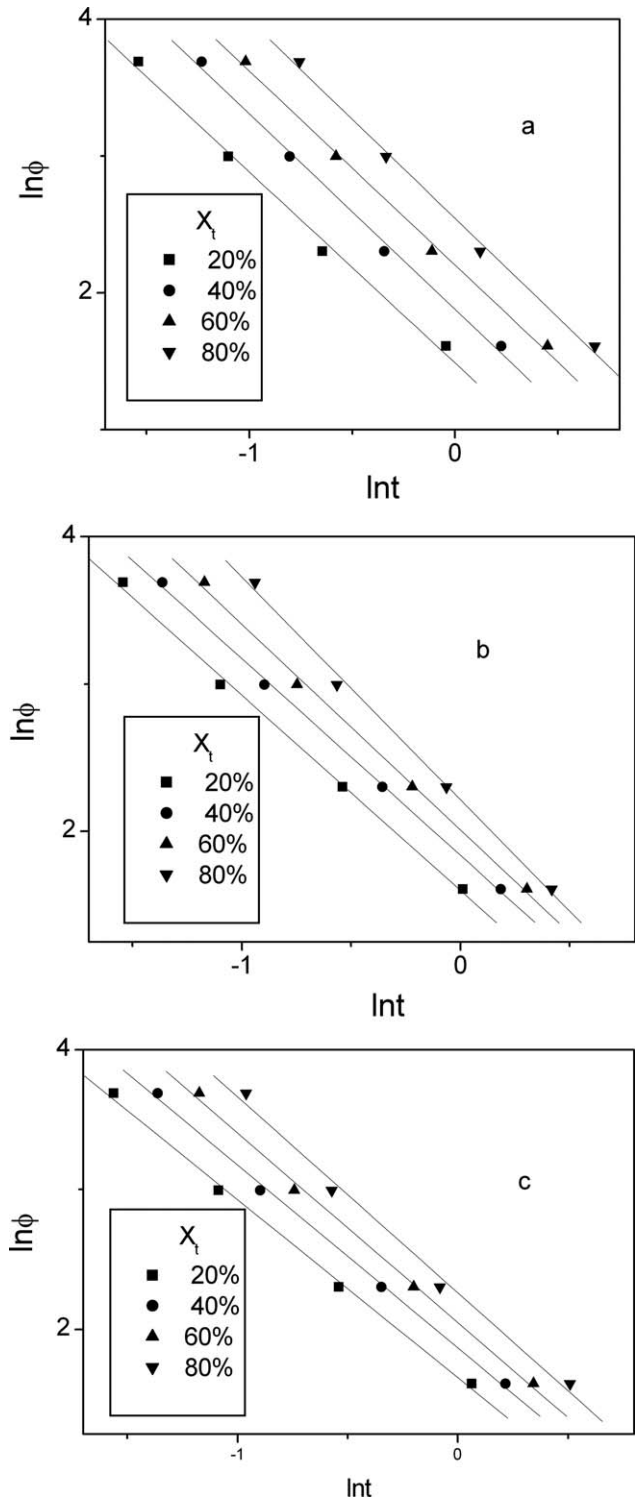

Figure 10 Plots of $\ln\Phi$ versus lnt for different degrees of crystallinity: (a) PP, (b) P1, and (c) P2.

TABLE IV
Nonisothermal Crystallization Parameters for PP and PP/Nano-PPSQ Composites at Different Degrees of Crystallinity

Samples	X_t (%)	α	$F(T)$	ΔE(KJ/mol)
PP	20	1.40	4.43	197.58
	40	1.43	6.56	
	60	1.42	9.05	
	80	1.45	12.73	
P1	20	1.27	5.22	218.22
	40	1.31	6.47	
	60	1.36	7.75	
	80	1.40	9.60	
P2	20	1.32	4.95	211.05
	40	1.33	6.28	
	60	1.40	7.46	
	80	1.51	9.16	

Kissinger method

Kissinger model provides the following expression for the determination of the activation energy in nonisothermal condition.

$$d[\ln(\Phi/T_p^2)]/d(1/T_p) = -\Delta E/R \quad (8)$$

where T_p is the crystallization peak temperature, R is the universal gas constant, and ΔE is the activation energy.[21] The plots of $[\ln(\Phi/T_p^2)]$ as function of $1/T_p$ using eq. (8) for PP and nanocomposites are presented in Figure 11(a–c). The values of ΔE are given in Table IV. Crystallization of polymer results from the alignment of mobile polymer chains. In the case of nanocomposites, the regions of the polymer chain are immobilized on the surface of nano-PPSQ particles due to the adherence of two surfaces. The regions of the PP chain attached onto the surface of nano particle reduced the mobility of PP chains during crystallization process, resulting in a higher activation energy as shown in Table IV.

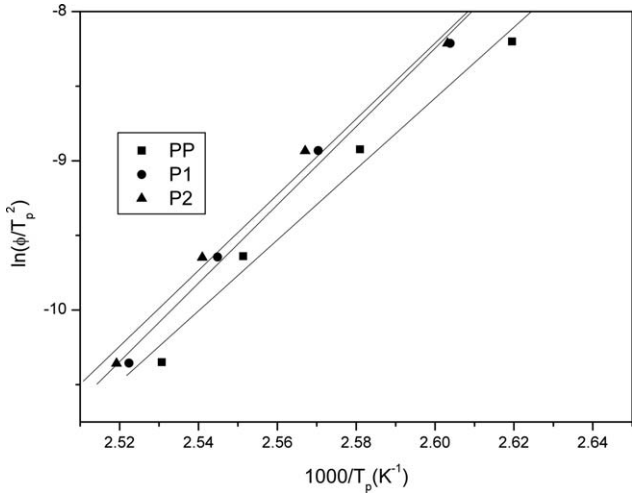

Figure 11 Plots of $[\ln(\Phi/T_p^2]$ as a function of $1/T_p$ for the three samples PP, P1, and P2.

CONCLUSIONS

The nano spherical poly(phenylsilsesquioxane) particles were prepared and characterized. The morphology of the prepared particles showed that the spheres were about 100 nm. The analysis of the PP/nano-PPSQ composite structure showed that the particles were well dispersed in PP. Because of the outdiffusion of the volatile decomposition products and the oxygen diffusion in the composites are impeded by spherical particles or decomposition products of them, the thermal stability of PP can be enhanced, and the T_{10} and T_{50} of the composites with wt 5% nano-PPSQ are improved about 59.6°C and 29.2°C, respectively. The crystallite size perpendicular to the crystalline planes like (0 4 0), (111), (041) of the nanocomposites is smaller than that of pristine PP and this indicated that nano particles have heterogeneous nucleus effect on pure PP. The Avrami analysis modified by Jeziorny and a method developed by Mo were successful in describing the nonisothermal crystallization process of PP and the PP/nano-PPSQ composites. Because the polymer chains are immobilized on the surface of nano-PPSQ particles, addition of the nano particles results in higher activation energy.

References

1. Paul, D. R.; Robeson, L. M. Polymer 2008, 49, 3187.
2. Bakar, M.; Kostrzewa, M.; Okulska-Bozek, M.; Jacewicz, E. J Appl Polym Sci 2011, 119, 752.
3. Yoshimoto, A.; Takahiro, G. Prog Polym Sci 2004, 29, 149.
4. Anna, A.; John, N. H. J Mater Chem 2003, 13, 3122.
5. Li, G. Z.; Wang, L. C.; Ni, H. L.; Charles, U. P. J. J Inorg Organ Polym 2001, 11, 123.
6. Takahashi, K.; Tadanaga, K.; Matsuda, A.; Hayashi, A.; Tatsumisago, M. J Sol-Gel Sci Techn 2007, 41, 217.
7. Alexandre, M.; Dubois, P. Mater Sci Eng 2000, 28, 1.
8. Nath, D. C. D.; Bandyopadhyay, S.; Yu, A. B.; Blackburn, D.; White, C. J Appl Polym Sci 2010, 115, 1510.
9. Hah, H. J.; Kim, J. S.; Jeon, B. J.; Koo, S. M.; Lee, Y. E. Chem Commun 2003, 14, 1712.
10. Ma, C.; Kimura, Y. Polym J 2002, 34, 709.
11. Mori, H.; Miyamura, Y.; Endo, T. Langmuir 2007, 23, 9014.
12. Qin, H. L.; Zhang, S. M.; Zhao, C. G.; Feng, M.; Yang, M. S.; Shu, Z. J.; Yang, S. S. Polym Degrad Stab 2004, 85, 807.
13. Ni, Q. L.; Fan, J. Q.; Dong, J. Y. J Appl Polym Sci 2009, 114, 2180.
14. Perrin-Sarazin, F.; Ton-That, M. T.; Bureau, M. N.; Denault, J. Polymer 2005, 46, 11624.
15. Xu, W. B.; Liang, G. D.; Zhai, H. B.; Tang, S. P.; Hang, G. P.; Pan, W. P. Eur Polym J 2003, 39, 1467.
16. Avrami, M. J. J Chem Phys 1941, 9, 177.
17. Jeziorny, A. Polymer 1978, 19, 1142.
18. Qin, J.; Chen, X. L.; Yu, J.; Wang, Y.; Tian, Y. Z.; Wu, S. J Appl Polym Sci 2010, 117, 1047.
19. Ozawa, T. Polymer 1971, 12, 150.
20. Liu, T. X.; Mo, Z. S.; Wang, S. G.; Zhang, H. F. Polym Eng Sci 1997, 37, 568.
21. Kissinger, H. E. J Res Natl Stand 1956, 57, 217.